Experimental measurement of velocity correlations for two microparticles in a plasma with ion flow

Amit K. Mukhopadhyay and J. Goree

Department of Physics and Astronomy, The University of Iowa, Iowa City, Iowa 52242, USA

Velocity correlations are measured in a dusty plasma with only two microparticles. These correlations allow a characterization of the oscillatory modes and an identification of the effects of ion wakes. Ion wake effects are isolated by comparing two experiments with the microparticles aligned parallel vs perpendicular to the ion flow. From records of microparticle velocities, the one- and two-particle distribution functions f_1 and f_2 are obtained, and the two-particle correlation function $g_2 \equiv f_2 - f_1 f_1$ is calculated. Comparing the two experiments, we find that motion is much more correlated when the microparticles are aligned with the ion flow and the character of the oscillatory modes depends on the ion flow direction due to the ion wake.

I. INTRODUCTION

We investigate a dusty plasma [1,2] that has the simplest possible configuration with collective effects among microparticles: It has only two microparticles, which are confined by electric forces in the plasma. The microparticles are micron-size polymer spheres, and the plasma in which they are immersed includes flowing ions, neutral gas atoms, and electrons. The microparticles, also known as dust particles, become negatively charged by absorbing more electrons than ions from the plasma [3]. The charge is large, typically thousands of elementary charges, but the charge-to-mass ratio is tiny compared to that of a proton. The two microparticles interact directly with one another through a Coulomb repulsion that is partially screened by the electrons and ions. They also interact indirectly by modifying the trajectories of the flowing ions, which alters the screening of the plasma and thereby affects the other microparticle. The latter phenomenon is the so-called wake effect.

The wake effect in dusty plasmas has been studied theoretically [4–26] and in experiments [27–41]. The experiments reveal a tendency for microparticles to align with the ion flow. This alignment is explained by the focusing of the ions downstream of the microparticle, creating a positive space charge region that can attract another negatively charged microparticle. In this way, microparticles tend to align themselves in strings parallel to the ion flow.

In addition to a tendency for microparticles to align, the wake effect has another consequence that has been much studied: a nonreciprocal interaction between microparticles [6,7,9]. Energy in the directed ion flow can be converted into kinetic energy of the microparticles. It has been observed that the wake of the upper particle affects the motion of the lower particle significantly, but the reverse effect is so small as to be negligible [30,31].

Due to their small charge-to-mass ratio, microparticles that are confined have oscillatory modes with a low frequency of only a few hertz [43–45]. These oscillations, which will be one of our main topics, have two causes. The confining forces provided by the shape of the sheath is one cause, and it can result in oscillations of just one particle. When a second particle is added, the other cause of the oscillations appears, and that is the interparticle interaction, including both the mutual repulsion of the microparticles themselves and the

modification by the wake effect. Different modes can have different characters, for example, the microparticles can move together in what is termed center-of-mass motion, or they can move oppositely.

Many dusty plasma experiments have been performed with large clusters of microparticles that are thousands to only a few in number [44–52]. Fewer experiments have been reported with only two microparticles, including Refs. [32,33,38,39,41,53–57]. These experiments with just two microparticles have a special value because a system with two particles is the smallest one that can include interactions among them. These experiments include an experimental estimation of microparticle charge [34,38], studies of the bistability of the orientation of the microparticle pair with respect to the direction of the ion flow [32], and the oscillatory modes [33–35,58]. Wake effects tend to greatly influence experiments with only two microparticles, which has been investigated theoretically as well [6,59–61].

Experimental techniques that have been used to study a system of two microparticles include recording the trajectories of two microparticles. Here we will also record trajectories of both microparticles in a two-particle system. However, we will then use an analysis method that we recently introduced [62] based on two-particle distributions and correlation functions.

To isolate the effects of the ion wake, we compare two experiments: one with the two microparticles aligned parallel to the ion flow and the other aligned perpendicularly. In our experiments, the ion flow is always directed downward onto a horizontal lower electrode so that we will often use the terms *vertical* and *horizontal* alignments to refer to the *parallel* and *perpendicular* directions with respect to the ion flow. The two experiments use different confining forces to select whether the microparticles are aligned horizontally or vertically. For the horizontally aligned situation the wake has the same effect on both the microparticles, but for vertical alignment the situation becomes asymmetric. Our horizontally aligned experiment was reported previously [62]; here we present those results again, along with the results of our vertical experiment, to allow a comparison for identifying effects of the ion wake on the microparticles' motion and oscillatory modes.

Our experimental technique for analyzing the motion of the microparticles [62] centers on the determination of a velocity correlation function g_2. This correlation function is motivated

by the Meyer cluster expansion [64–66], which includes a one-particle distribution function f_1 and a two-particle distribution function f_2. These distribution functions can be determined experimentally by histograms of observations of velocities. The correlation function for the one-dimensional system is defined as

$$g_2(v_{x,\alpha},v_{x,\beta}) = f_2(v_{x,\alpha},v_{x,\beta}) - f_1(v_{x,\alpha})f_1(v_{x,\beta}), \quad (1)$$

where α and β identify the two particles. Comparing this correlation function for the horizontally vs vertically aligned experiments will reveal the effects of the wake induced forces. The correlation function is also useful for identifying the nature of the oscillatory modes.

II. EXPERIMENT AND ANALYSIS

We performed experiments with a partially ionized argon plasma produced by applying radio frequency (rf) power to a horizontal electrode. The vacuum chamber, which was grounded, served as the other electrode. The gas pressure was 13.5 mTorr. The 13.56 MHz rf power was capacitively coupled to the lower electrode so that a significant negative dc bias could develop on this electrode.

Two melamine formaldehyde microparticles were electrically levitated in the plasma sheath above the horizontal electrode. The size of the microparticles was 4.81 μm, and they experienced a gas drag with a coefficient [67] of 4.5 s^{-1}. We introduced them by agitating a dispenser above the plasma. The dispenser had a single small opening of ≈ 0.07 mm. Using a camera to image the microparticles, we observed how many were introduced. If there were more than two, we eliminated the excess by briefly extinguishing the plasma in a series of pulses.

To select vertical vs horizontal alignment of the microparticles, we shaped the sheath above the lower electrode. We performed this by arranging metal objects on the lower electrode and changing the sheath thickness by adjusting the rf voltage. To attain horizontal alignment, we arranged rectangular metal blocks on the lower electrode so that there was a shallow rectangular opening in the center of their pattern as shown in the Supplemental Material of Ref. [62], and we used a high peak-to-peak rf voltage of 180 V with a dc self-bias of −89 V. For vertical alignment, we stacked two metal washers on the center of the electrode as shown in Fig. 1, and we used a lower peak-to-peak rf voltage of 60 V and a correspondingly lower dc self-bias of −16 V. The washers had an inner diameter of 2 cm and a total thickness of 1 cm. A lower rf voltage results in a lower plasma density and a correspondingly thicker sheath; this greater thickness of the sheath gives it a more rounded shape as it conforms to the contours of the metal surfaces on the electrode. A gently rounded depression in the sheath promotes a horizontal alignment, whereas a sharper deeper profile for the sheath favors a vertical alignment. Previous experimenters using two microparticles found that it was possible to make a transition between horizontal and vertical alignment by adjusting the rf voltage within a narrow range [32]; we used more extreme rf voltages to avoid this transition so that we always had a stable arrangement of the two microparticles.
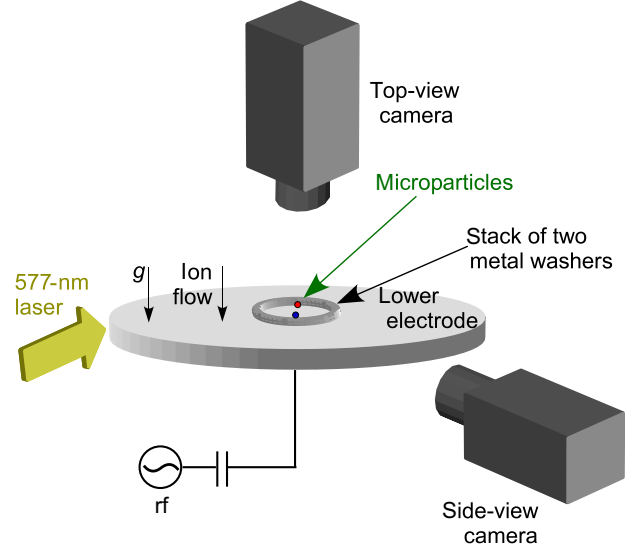

FIG. 1. (Color online) Experimental setup. Two microparticles were electrically levitated in the sheath above the lower electrode. We shaped this sheath with a stack of two metal washers as shown to provide vertical microparticle alignment and an arrangement of metal blocks for horizontal alignment. Microparticles were illuminated by a laser and were imaged by either a side-view or a top-view camera. The vacuum chamber, not shown here, serves as the grounded electrode.

The two experiments have different symmetries with respect to the microparticle charges and the ion wakes. Horizontally aligned particles are exposed to the same plasma conditions so that their charges will be the same. Moreover, each microparticle's wake affects the other microparticle equally. Vertically aligned particles, however, are levitated by an electric field that is stronger for the lower microparticle so that the two have different charges as was reported in Refs. [34,35,38,68–70]. In the experiment by Carstensen *et al.* [38], it was estimated that for their experimental conditions, the lower microparticle particle had a charge only 78% as large, i.e., $Q_\beta/Q_\alpha = 0.78$. Also, the wake of the *upper* microparticle is the only wake that is positioned where it can influence the other microparticle as shown by Melzer [31]. Because of these differences in the symmetry, any difference in the two experiments must be due to the wake effect or the unequal charging with vertical alignment. We can further narrow the possible causes by dismissing unequal charging if we detect a particular signature of the wake effect, such as an increase in energy as can be caused by the nonreciprocal wake interaction or an enhanced tendency of a lower microparticle to track the upper one.

We illuminated the microparticles with a laser and imaged them with a high-speed video camera (see Fig. 1). A 577 nm laser beam was shaped into a sheet using a cylindrical lens. The laser power was small enough that the microparticles were not visibly disturbed. The camera was a Phantom v5.2, fitted with a 105 mm focal length lens and operated at 100 frames per second. The camera was mounted differently to view from the top or side for the horizontal and vertical alignment experiments, respectively. Image sequences from the experiments are shown in Figs. 2(c) and 2(d). Using image analysis methods [71,72] we measure the coordinates of a
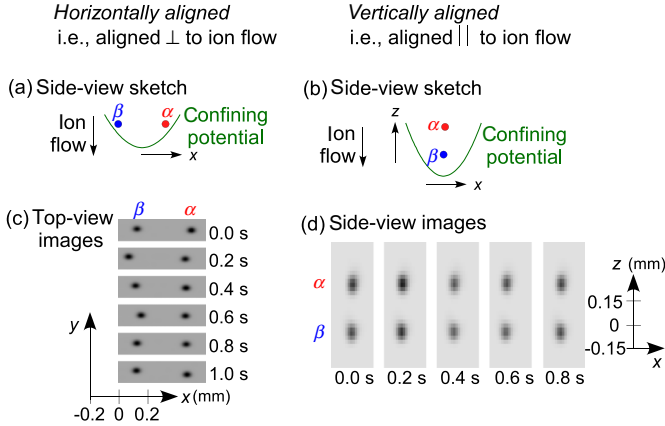
FIG. 2. (Color online) Horizontal and vertical alignments of microparticles. In (a) and (b) we sketch the shape of the sheath above the lower electrode and the resulting alignment of the microparticles. Sequences of images recorded by the camera, (c) and (d), show the actual alignment and the small displacements due to random motion. We analyze these images to obtain the time series of microparticle positions. Panels (a) and (c) are reported in Ref. [63].

microparticle in each video frame so that we can track them in successive images and can calculate their velocity. This yields the time series of velocities for each microparticle, which are used for all our further analyses.

Our experiment with the vertically aligned microparticles differs from previous experiments in both the way the experiment was performed and the analysis that is used. For example, Melzer used laser manipulation to perturb a vertically aligned pair of microparticles to observe an instability arising from the wake effect [31]. Kong and co-workers [34,35] and Carstensen *et al.* [38] studied oscillatory modes for two vertically aligned particles while manipulating them by modulating the voltage on the lower electrode. To study the oscillatory modes we do not perform any manipulation but rely instead on the natural Brownian motion, which can be enhanced by wake-driven instabilities. Any oscillatory modes will be present in this natural motion. Another difference is that we performed both vertically and horizontally aligned experiments to allow a direct comparison. A final difference is that our analysis relies mainly on our correlation function.

We will identify the modes using several diagnostics, including a calculation of the spectrum of the oscillatory modes. The spectra are calculated separately for the two particles. This is performed by computing the modulus of the fast Fourier transform (FFT) of the velocity time series $v_{x,\alpha}(t)$ and $v_{x,\beta}(t)$.

Our main results will be distribution functions f_1 and f_2 and correlation functions g_2. We obtain these from the velocity time series. We consider each data point in the time series as an independent observation, and we build histograms of these observations. We determine f_2 jointly for the two particles but f_1 separately for each particle. We then use Eq. (1) to compute g_2.

A variation on this correlation-function analysis is to frequency filter the velocity time series before calculating the distribution functions and the correlation function. This filtering allows an isolation of a particular oscillatory mode. This is done by performing an FFT of the $v_{x,\alpha}(t)$ time series,

for example, then multiplying by a filter function, and finally performing a reverse FFT. The filter function was a simple rectangle so that frequencies within a specified bandwidth were weighted equally, whereas those outside the bandwidth were eliminated.

III. RESULTS

Our main results for the comparison of horizontal vs vertical alignment are presented in Sec. III A where we rely on measurements of the horizontal velocity component v_x, which is perpendicular to the ion flow. Additionally, in Sec. III B we present results for v_z, which is parallel to the ion flow; the latter results are only for the vertically aligned experiment, which allowed this measurement because of camera configuration.

A. v_x motion perpendicular to the ion flow

1. Correlations

The two microparticles tend to move together regardless of whether they are aligned perpendicularly or parallel to the ion flow, but in the latter case, this tendency is stronger. This is seen in the velocity time series Figs. 3(a) and 3(b) where $v_x(t)$ for the two particles are nearly the same. This comovement of particle motion is more pronounced for vertical alignment, i.e., alignment *parallel* to the ion flow as seen by the abundance of overlapping data points in Fig. 3(b). It is less pronounced for horizontal alignment, i.e., alignment *perpendicular* to the ion flow, which allows some instances when the two microparticles actually move in opposite directions, such as at $t = 1.2$ s in Fig. 3(a). This difference in the results for microparticle alignment parallel vs perpendicular to the ion flow must be attributed to either the ion wake or the unequal charging of the two microparticles when they are vertically aligned. Of these two possibilities, only the wake effect can account for a greater tendency of the particles tracking one another when they are vertically aligned.

2. Heating

The heating effect due to the ion flow is more substantial for alignment parallel to the ion flow, i.e., for the vertically aligned configuration. This is seen by comparing Figs. 3(a) and 3(b) where the velocities are typically twice as large for vertical alignment in Fig. 3(b). This is verified by comparing the one-particle distribution functions $f_1(v_x)$ in Figs. 3(c) and 3(d) where the distributions are broader for the alignment parallel to the ion flow in Fig. 3(d). The root-mean-square velocity is $v_{x,\alpha}^{\text{th}} = v_{x,\beta}^{\text{th}} = 0.28$ mm/s for perpendicular alignment but a much larger $v_{x,\alpha}^{\text{th}} = 0.58$ and $v_{x,\beta}^{\text{th}} = 0.77$ mm/s for parallel alignment.

Because of symmetry, one might expect that the heating effect would act identically on the two microparticles when they are horizontally aligned but not vertically. We find that this is indeed true by comparing the widths of the distributions in Figs. 3(c) and 3(d). For vertical alignment, however, the lower microparticle is heated to a greater extent. The latter finding is similar to the case for a bilayer of many microparticles where the lower layer has been observed to have a higher kinetic temperature [73], which was attributed to an instability arising from the ion flow [6,7].
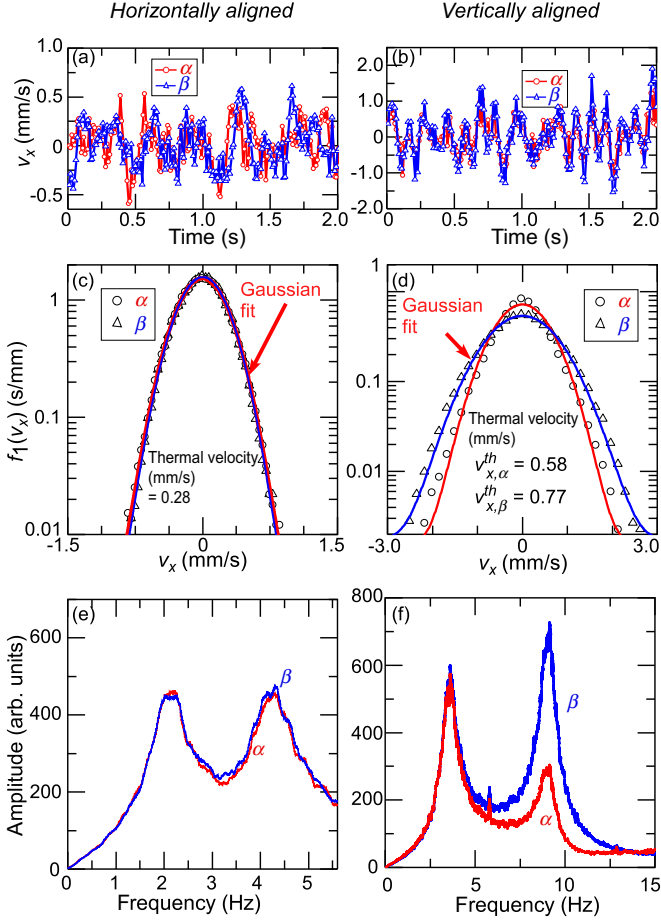
FIG. 3. (Color online) Velocity data. Note that scales are different for horizontal vs vertical alignment. Time series of velocities show how the two microparticles tend to move together, more so when they are vertically aligned (b) than when they are horizontally aligned (a). These velocity time series are used to obtain all other results, including the one-particle distribution functions f_1, (c) and (d). For vertical alignment (d) the amplitudes of v_x are larger than for horizontal alignment (c), and the lower microparticle has the largest amplitudes. Frequency spectra (i) and (j), computed as the modulus of the FFT of $v_x(t)$, show two distinctive peaks corresponding to two modes. Frequencies are generally higher for vertical alignment due to the narrower configuration of the confining potential. Data in (c) and (e) for particle α were previously reported in Ref. [63].

The one-particle velocity distributions f_1 are mostly Gaussian. This is seen by the fits in Figs. 3(c) and 3(d). However, there is a detectable fat tail for the lower microparticle for vertical alignment [74].

3. f_2 and g_2

Results for f_2 are presented in Figs. 4(a) and 4(b). For vertical alignment in Fig. 4(b), the contours for f_2 have a prominent tilt, and they are compressed so that the observations fall mainly on a thick tilted line in the velocity space $v_{x,\alpha}$ vs $v_{x,\beta}$. This is entirely different from the nearly circular pattern for the experiment with horizontal alignment, Fig. 4(a). We can interpret these tilted compressed contours in Fig. 4(b) as an indication that, when the microparticles are vertically aligned,
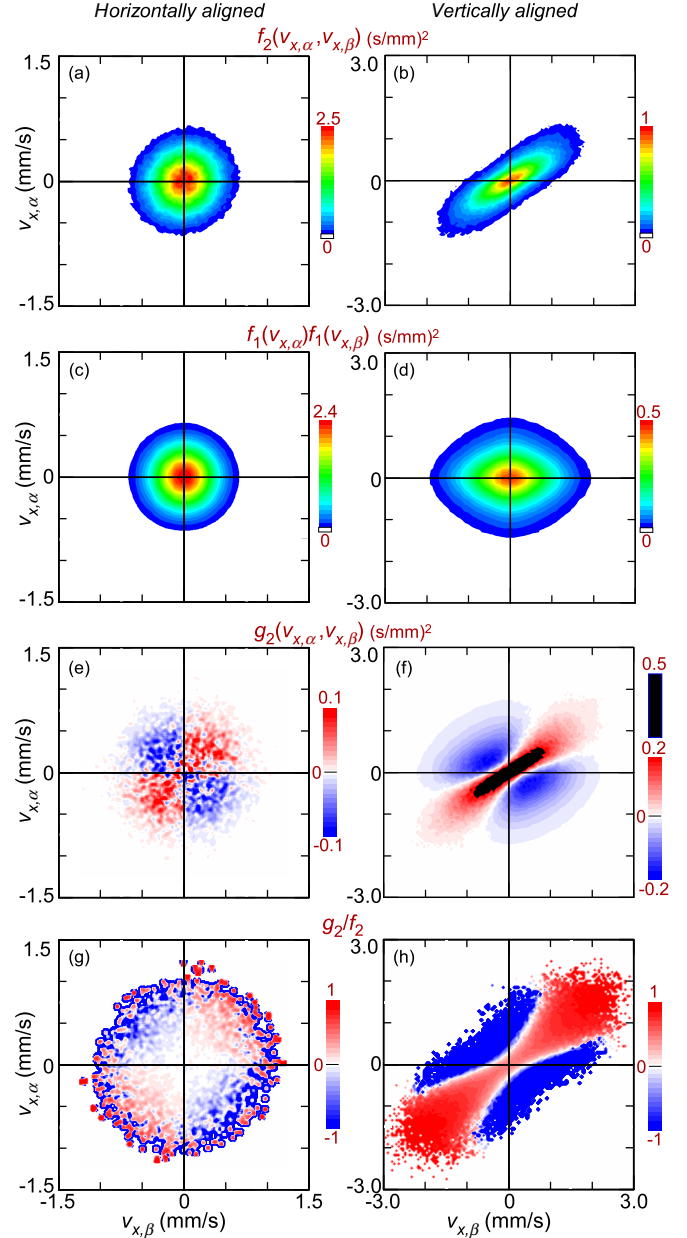

FIG. 4. (Color online) Two-particle velocity distribution f_2 and correlation function g_2. The axes of these graphs are the x-component velocities of the two microparticles. We find that f_2 is slightly noncircular for horizontal alignment but highly noncircular for vertical alignment. Using Eq. (1), we subtract the product $f_1 f_1$ in (c) and (d) to yield the correlation function g_2 in (e) and (f). Red (the top of the color bar) indicates a positive correlation where the two microparticles move together, whereas blue (the bottom of the bar) is for the negative correlation where they move oppositely. Correlations are much more distinct for vertical alignment in (f) as compared to horizontal alignment in (e). We normalize g_2 by f_2 in (g) and (h) to better show that the most significant correlations are those at higher velocities. Data shown in (a), (c), (e), and (g) were previously reported in Ref. [63].

they closely track one another in their motion, moving almost as if they were one.

To help understand this interpretation of the contours of f_2, we consider some hypothetical examples. First, suppose
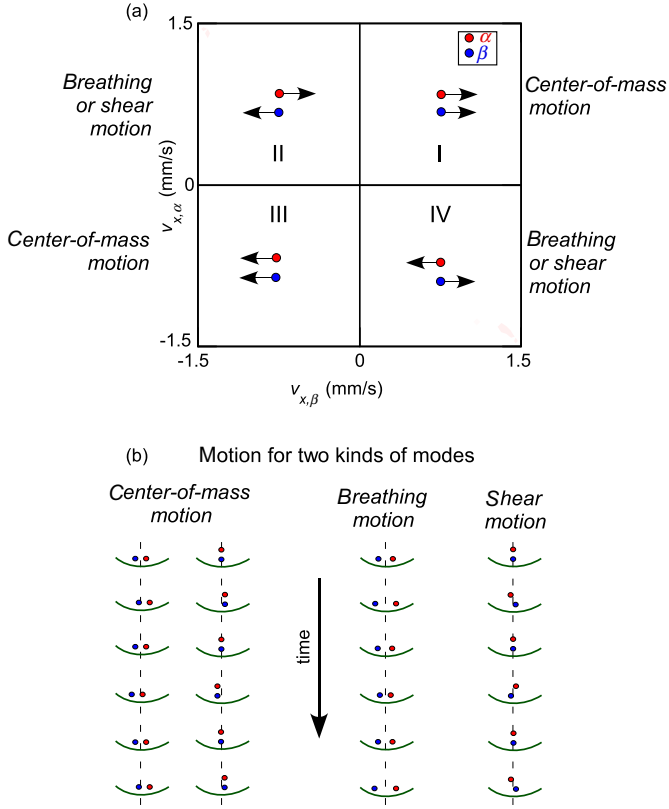
FIG. 5. (Color online) Sketch of microparticle motion associated with possible oscillatory modes. In snapshot (a), we label the kind of motion in the quadrants of Figs. 4 and 6. In time series (b), we distinguish center-of-mass motion from another possible mode, which is a breathing mode for horizontal alignment and a shear motion for vertical alignment.

that the two particles behave identically and are completely uncorrelated. In this case, the f_2 contours should be completely circular as is nearly the case for Fig. 4(a) for alignment perpendicular to the ion flow. Second, suppose that the two particles behave identically so that they precisely move together $v_{x,\alpha}(t) = v_{x,\beta}(t)$; in this case, f_2 would be a thin line tilted precisely at 45°. Third, suppose that the two particles again move together, except that the lower microparticle has larger movements $v_{x,\beta} = 1.3v_{x,\alpha}$; then the plot of f_2 would again be a thin line but would be tilted by an angle less than 45°. Finally, suppose that the motion is as in the last case but not perfectly correlated; then the contours of f_2 would be broader than a line and would be tilted at less than 45°; this is like our result in Fig. 3(b) for alignment parallel to the ion flow. Thus, this series of examples leads us to interpret the contour shape in Fig. 3(b) as evidence that the two particles tend to move together without perfect correlation and with a larger amplitude for the lower one.

One of our main results is the comparison of the velocity correlation functions g_2 for the two experiments in Figs. 4(e) and 4(f) computed using Eq. (1). Comparing the two experiments, we find both a similarity and a difference.

The similarity is that, for both experiments, the two microparticles show a tendency to move together. This can be seen from the abundance of positive correlations in quadrants

I and III and negative correlations for quadrants II and IV. This would be expected when correlations are present because, in quadrants I and III, the two particles are moving in the same direction at the same time.

A difference in the correlation function g_2 for the two experiments can be seen in the distinctiveness of the features of g_2. For vertical alignment, we note that the positive values of g_2 are concentrated in a distinctive tilted line. This observation is consistent with a strong tendency for the microparticles to move together when they are aligned parallel to the ion flow, which we attribute to the wake effect.

One limitation of g_2, as a tool for understanding correlations, is that it will tend to have large values for velocities near zero, even if particles do not really move together very often. This is so because g_2 is weighted by the abundance of particles in a portion of velocity space and there is a great abundance of microparticles at near-zero velocities. To avoid this limitation, we calculate the ratio g_2/f_2 in Figs. 4(g) and 4(h).

We find that g_2/f_2 is completely different for the two experiments. For alignment *perpendicular* to the ion flow in Fig. 3(g), correlations are significant mainly for high speeds > 0.85 mm/s, i.e., speeds $> 3v^{th}$. For alignment *parallel* to the ion flow, Fig. 4(h), there is significant correlation at high and low speeds, and the contours of g_2/f_2 have a distinctive pattern. This pattern has positive correlations concentrated on the thickened tilted line.
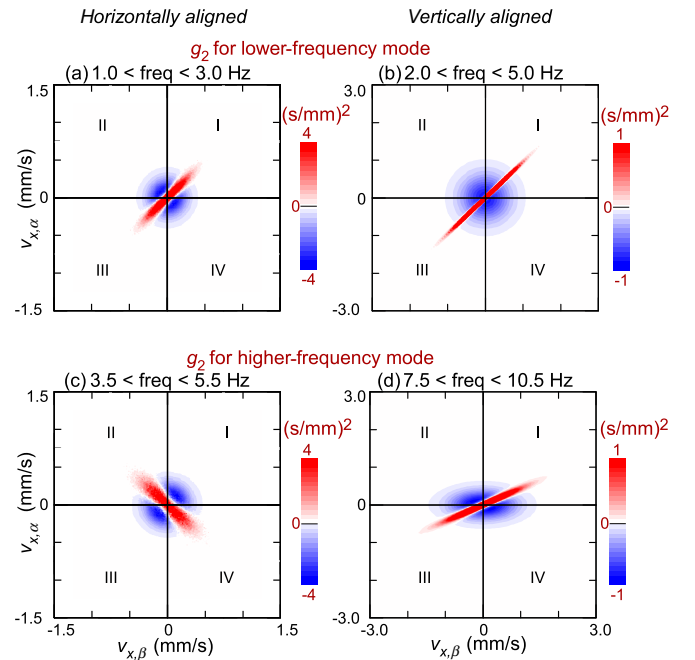

FIG. 6. (Color online) Frequency-filtered correlation functions for identifying modes. For vertical alignment, which is dominated by the wake effect, both the (b) low-frequency and the (c) high-frequency modes have a center-of-mass character as indicated by the upward slope of the positive-correlation feature. For horizontal alignment, only the lower-frequency mode (a) has a center-of-mass motion, whereas the higher mode (c) has a breathing motion as indicated by a downward slope of the positive-correlation feature. Data shown in (a) and (c) were previously reported in Ref. [63].
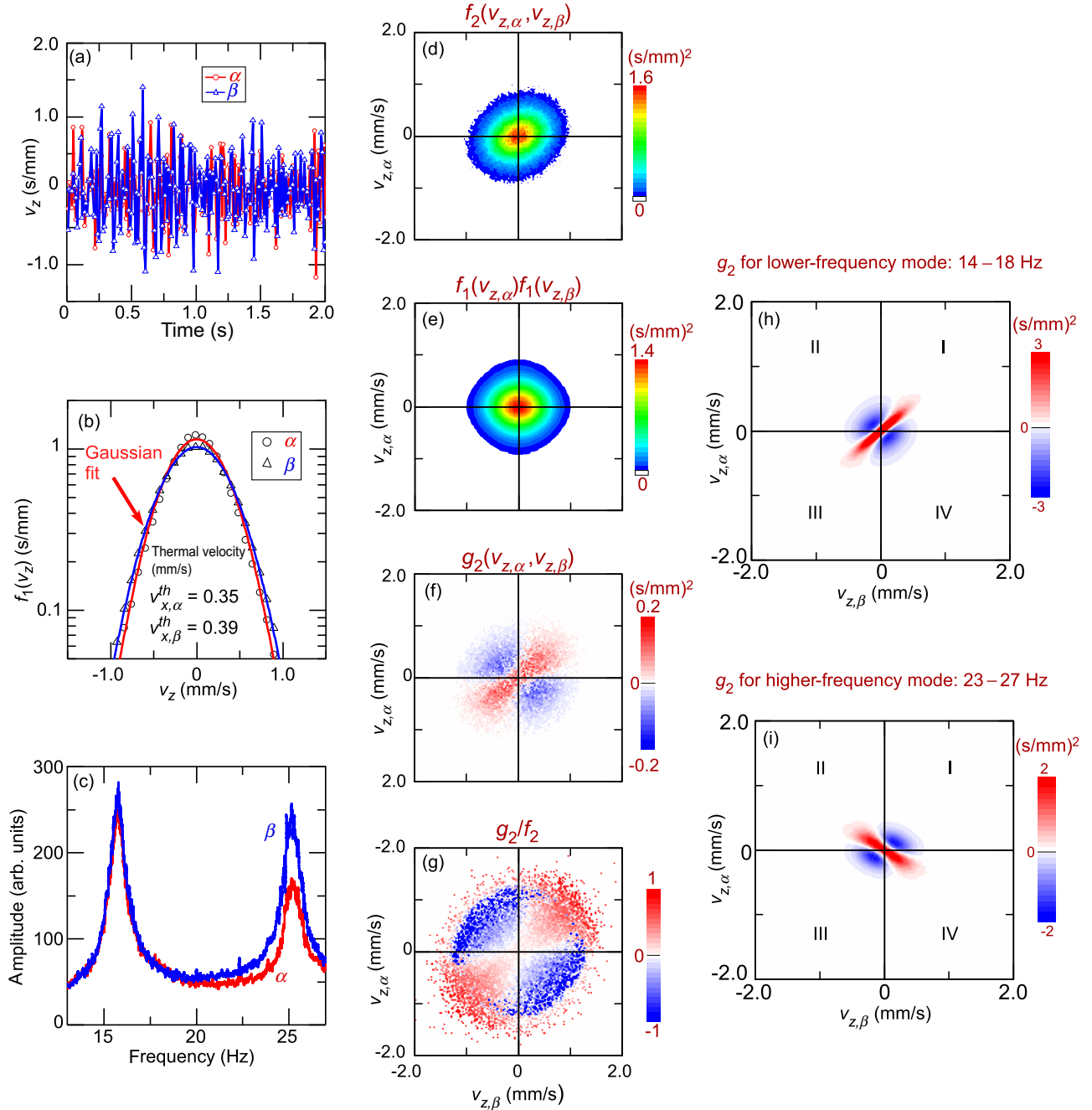
FIG. 7. (Color online) Results for the vertical v_z motion for the vertically aligned configuration. For vertical alignment, v_x and v_z have many of the same signatures: The amplitude is larger for the lower particle as seen in the velocity time series (a) and more clearly in the one-particle distribution function f_1 in (b) and its product in (e); the upper frequency mode has a higher amplitude for the lower particle as seen in the frequency spectrum (c), and the two-particle distribution function f_2 in (d) is noncircular, causing the correlation function g_2 to have distinctive features in (f) and (g). However, motion in the z direction has different signatures in all respects that involve the modes: We find that the modes for v_z motion have higher frequencies (c) as compared to the x motion in Fig. 3(f), and we find that the highest-frequency mode has a breathing character as indicated by the downward slope of the positive-correlation feature in the frequency filtered g_2 data.

4. Modes

The frequency spectra in Figs. 3(e) and 3(f) show that in both experiments there are *two* main modes of oscillation. However, these two modes are not the same for vertical and horizontal alignments. The mode frequencies are higher for vertical alignment (3.65 and 9.0 Hz) and lower for horizontal alignment (2.1 and 4.2 Hz). These frequencies depend on the alignment because the scale lengths of confining forces and interparticle forces are different for the two experiments.

Examining the frequency spectra, we find that the effects of the ion wake are more prominent for the high-frequency peak in the spectra when the microparticles are vertically

aligned, i.e., at 9.0 Hz, Fig. 3(f). At this frequency, the lower microparticle has a higher amplitude. This difference must be due to the wake effect. At the lower frequency, the two particles have about the same amplitude, suggesting that the wake has less of a role in this lower-frequency mode. For horizontal alignment, Fig. 3(e), based on symmetry we expect that the two particles will oscillate the same way, and their overlapping spectra confirm that this is so.

To help interpret the graphs of g_2, we illustrate some possible modes in Fig. 5. In the velocity space $v_{x,\alpha}$ vs $v_{x,\beta}$, there are four quadrants, Fig. 5(a). In quadrants I and III, there is some character of center-of-mass motion [44,45] where the two particles move in the same direction at the same time. In quadrants II and IV, the two microparticles move in opposite directions at a given time; this type of mode can be described as breathing motion [44,45] (for horizontal alignment) or shear motion (for vertical alignment). The spatial-temporal development of these possible oscillatory modes is sketched in Fig. 5(b).

To identify the modes we use frequency-filtering method described in the Supplemental Material of [62]. For g_2, this filtering yields Fig. 6. For vertical alignment, both modes have a center-of-mass character, and a shear motion mode is not observed. This conclusion is drawn from Figs. 6(b) and 6(d) where the positive correlations are in quadrants I and III for both frequency ranges. However, for horizontal alignment, only one mode has a center-of-mass character, whereas the other corresponds to breathing motion, which is demonstrated by Figs. 6(a) and 6(c).

Although the two dominant modes for the vertically aligned experiment both have center-of-mass character, they differ in several ways. As we established from the spectra, the two modes have different frequencies, and the lower particle has a larger amplitude for the higher frequency, whereas both microparticles have the same amplitude for the lower frequency. The same tendencies are seen in the filtered g_2 data by comparing Figs. 6(b) and 6(d). At the higher frequency, the concentration of high correlations on a thick line that is not tilted at 45° indicates that the two particles have different amplitudes in their motion even as they generally move in the same direction at the same time. At the lower frequency, the thick line is at 45°, indicating the same amplitude for both particles at this frequency.

B. v_z motion parallel to the ion flow

The measurements reported above for v_x are our primary results. In addition, we also measured v_z in our vertically aligned experiment as we report next. A portion of the time series of the vertical velocity v_z, the distribution functions f_1 and f_2, and the correlation function g_2 are presented in Fig. 7. In general, v_x and v_z are not correlated for a given microparticle [75].

We find that the microparticle kinetic energy for the vertical motion $m v_z^2/2$ is less than for the horizontal motion $m v_x^2/2$. This is seen by comparing the thermal velocities as marked in Figs. 3(d) and 7(b). The ratio of the horizontal to vertical thermal velocities is about 1.63 and 1.95 for the upper and lower microparticles, respectively, so that the ratio of the kinetic energies is correspondingly 2.66 and 3.82. We interpret this result as an indication that the wake effect does not partition the energy equally into vertical and horizontal

components of the particle motion, but instead, it pumps several-fold more energy into the horizontal motion.

As with the horizontal motion, the vertical motion has larger velocities for the lower particle than for the upper one. We find that the rms vertical velocity is 11% larger for the lower particle as compared to the upper particle. Again, we attribute this to the wake effect causing a greater heating of the lower microparticle.

The oscillatory modes in the vertical direction differ from those for the horizontal motion both in their frequencies and in their collective character. The mode frequencies for the vertical motion are 16 and 25 Hz as seen in Fig. 7(c), which are several times higher than for the horizontal motion. Although the two modes for horizontal motion both exhibited a center-of-mass character, we find that, for vertical motion only, the lower mode has a center-of-mass character as seen by the positive correlations in quadrants I and III in Fig. 7(h). The upper mode for vertical motion has a breathing character as seen by the positive correlations in quadrants II and IV in Fig. 7(i).

IV. CONCLUSIONS

We compare experiments with two microparticles aligned *parallel* or *perpendicular* to a downward ion flow. This comparison allows a study of the ion wake as well as the oscillatory modes. The ion flow was in the vertical direction toward a horizontal lower electrode that was fitted with metal surfaces to the shape sheath above it. In the two experiments, the microparticles had the same size, and most of the plasma conditions were the same, except that to achieve vertical alignment, we used a lower plasma density and a different shape for the confining surfaces on the lower electrode. When the particles were vertically aligned, i.e., aligned parallel to the ion flow, the lower particle was positioned directly in the wake of the upper particle, unlike the horizontally aligned experiment where neither of the microparticles were positioned downstream of the other. Any major differences in the particle motion for the two experiments can be attributed to the wake effect or the unequal microparticle charging. These two possibilities can be further narrowed if either a microparticle's energy is enhanced or the lower microparticle has an increased tendency to track the motion of the upper one; in these cases, the difference must be due to the ion wake.

We use our recently developed method with two-particle velocity distributions and correlations [62] to describe the random motion of the microparticles and their modes.

Effects both expected and unexpected arise from the ion wake as it influences the oscillatory motion of the particles. We expected that the wake effect could add random energy in a heating effect. It indeed does so as indicated by the higher velocities observed for the vertical alignment as compared to horizontal alignment as seen in Figs. 3(a)–3(d). We also expected, based on what is known about bilayers [73], that the heating would be strongest for the lower microparticle when vertically aligned, and this is also so. We had less reason to expect our other observations below.

One of our major observations is that the velocity correlation in the random motion has a much more distinct anisotropy in velocity space for vertical alignment as seen by comparing Figs. 4(c) and 4(d). This difference is attributed to the wake

effect's tendency to make the lower microparticle track the motion of the upper one.

Another of our observations is that the oscillatory modes depend on the microparticle alignment. To study the modes, we recalculate the correlation function g_2 with a limited frequency bandwidth. When the microparticles are aligned vertically, both modes have characteristics of center-of-mass motion as seen in Figs. 6(b) and 6(d) where the lower- and higher-frequency modes arise from confinement and the wake effect, respectively. The expected shear mode for vertical alignment is not observed. However, we find that, when the microparticles are aligned horizontally, only one of the modes is for center-of-mass motion (due to the confinement), whereas the other exhibits differential motion (mainly due to interparticle repulsion) as seen in Figs. 6(a) and 6(c).

[1] P. K. Shukla and A. A. Mamun, *Introduction to Dusty Plasma Physics* (Institute of Physics, Bristol, 2002).

[2] M. Bonitz, C. Henning, and D. Block, Rep. Prog. Phys. **73**, 066501 (2010).

[3] S. A. Khrapak *et al.*, Phys. Rev. E **72**, 016406 (2005).

[4] S. V. Vladimirov and M. Nambu, Phys. Rev. E **52**, R2172 (1995).

[5] F. Melandso and J. Goree, Phys. Rev. E **52**, 5312 (1995).

[6] A. Melzer, V. A. Schweigert, I. V. Schweigert, A. Homann, S. Peters, and A. Piel, Phys. Rev. E **54**, R46 (1996).

[7] V. A. Schweigert, I. V. Schweigert, A. Melzer, A. Homann, and A. Piel, Phys. Rev. E **54**, 4155 (1996).

[8] O. Ishihara and S. V. Vladimirov, Phys. Plasmas **4**, 69 (1997).

[9] V. A. Schweigert, I. V. Schweigert, A. Melzer, A. Homann, and A. Piel, Phys. Rev. Lett. **80**, 5345 (1998).

[10] G. Lapenta, Phys. Plasmas **6**, 1442 (1999).

[11] D. S. Lemons, M. S. Murillo, W. Daughton, and D. Winske, Phys. Plasmas **7**, 2306 (2000).

[12] G. Lapenta, Phys. Rev. E **62**, 1175 (2000).

[13] M. Lampe, G. Joyce, G. Ganguli, and V. Gavrishchaka, Phys. Plasmas **7**, 3851 (2000).

[14] J. E. Hammerberg, D. S. Lemons, M. S. Murillo, and D. Winske, IEEE Trans. Plasma Sci. **29**, 247 (2001).

[15] L.-J. Hou, Y.-N. Wang, and Z. L. Mišković, Phys. Rev. E **64**, 046406 (2001).

[16] S. V. Vladimirov, S. A. Maiorov, and O. Ishihara, Phys. Plasmas **10**, 3867 (2003).

[17] A. A. Samarian, S. V. Vladimirov, and B. W. James, JETP Lett. **82**, 758 (2005).

[18] R. Kompaneets, S. V. Vladimirov, A. V. Ivlev, V. Tsytovich, and G. Morfill, Phys. Plasmas **13**, 072104 (2006).

[19] A. Piel, Phys. Plasmas **18**, 073704 (2011).

[20] I. H. Hutchinson, Phys. Plasmas **18**, 032111 (2011).

[21] I. H. Hutchinson, Phys. Rev. Lett. **107**, 095001 (2011).

[22] I. H. Hutchinson, Phys. Rev. E **85**, 066409 (2012).

[23] P. Ludwig, W. J. Miloch, H. Kählert, and M. Bonitz, New J. Phys. **14**, 053016 (2012).

[24] O. S. Vaulina, I. I. Lisina, and K. G. Koss, Plasma Phys. Rep. **39**, 394 (2013).

[25] K. Qiao, J. Kong, Z. Zhang, L. S. Matthews, and T. W. Hyde, IEEE Trans. Plasma Sci. **41**, 745 (2013).

[26] S. Bhattacharjee and N. Das, Phys. Plasmas **20**, 113701 (2013).

[27] J. B. Pieper, J. Goree, and R. A. Quinn, Phys. Rev. E **54**, 5636 (1996).

[28] U. Mohideen, H. U. Rahman, M. A. Smith, M. Rosenberg, and D. A. Mendis, Phys. Rev. Lett. **81**, 349 (1998).

[29] K. Takahashi, T. Oishi, K.-i. Shimomai, Y. Hayashi, and S. Nishino, Phys. Rev. E **58**, 7805 (1998).

[30] A. V. Zobnin, A. P. Nefedov, V. A. Sinelshchikov, O. A. Sinkevich, A. D. Usachev, V. S. Filinov, and V. E. Fortov, Plasma Phys. Rep. **26**, 415 (2000).

[31] A. Melzer, Plasma Sources Sci. Technol. **10**, 303 (2001).

[32] V. Steinberg, R. Sütterlin, A. V. Ivlev, and G. Morfill, Phys. Rev. Lett. **86**, 4540 (2001).

[33] C. M. Ticos, P. W. Smith, and P. K. Shukla, Phys. Lett. A **319**, 504 (2003).

[34] J. Kong, T. W. Hyde, and J. Carmona-Reyes, IEEE Trans. Plasma Sci. **36**, 554 (2008).

[35] J. Kong, T. W. Hyde, B. Harris, K. Qiao, and J. Carmona-Reyes, IEEE Trans. Plasma Sci. **37**, 1620 (2009).

[36] C. Killer, A. Schella, T. Miksch, and A. Melzer, Phys. Rev. B **84**, 054104 (2011).

[37] O. Arp, J. Goree, and A. Piel, Phys. Rev. E **85**, 046409 (2012).

[38] J. Carstensen, F. Greiner, D. Block, J. Schablinski, W. J. Miloch, and A. Piel, Phys. Plasmas **19**, 033702 (2012).

[39] J. Carstensen, F. Greiner, and A. Piel, Phys. Rev. Lett. **109**, 135001 (2012).

[40] J. Kong, K. Qiao, J. Carmona-Reyes, A. Douglass, Z. Zhang, L. S. Matthews, and T. W. Hyde, IEEE Trans. Plasma Sci. **41**, 794 (2013).

[41] T. W. Hyde, J. Kong, and L. S. Matthews, Phys. Rev. E **87**, 053106 (2013).

[42] J. Kong *et al.*, Bull. Am. Phys. Soc., http://meetings.aps.org/Meeting/DPP13/Event/199842

[43] S. V. Vladimirov and N. F. Cramer, Phys. Scr. **58**, 80 (1998).

[44] A. Melzer, M. Klindworth, and A. Piel, Phys. Rev. Lett. **87**, 115002 (2001).

[45] T. E. Sheridan, Phys. Rev. E **72**, 026405 (2005).

[46] T. Trottenberg, D. Block, and A. Piel, Phys. Plasmas **13**, 042105 (2006).

[47] Y. Feng, J. Goree, and B. Liu, Phys. Rev. Lett. **100**, 205007 (2008).

[48] I. Pilch, T. Reichstein, and A. Piel, Phys. Plasmas **16**, 123709 (2009).

[49] J. D. Williams and J. Duff, Phys. Plasmas **17**, 033702 (2010).

[50] A. Schella, M. Mulsow, A. Melzer, H. Kählert, D. Block, P. Ludwig, and M. Bonitz, New J. Phys. **15**, 113021 (2013).

[51] Wen-Tau Juan, Zen-Hong Huang, Ju-Wang Hsu, Yin-Ju Lai, and Lin I, Phys. Rev. E **58**, R6947(R) (1998); Wen-Tau Juan, Ju-Wang Hsu, Zen-Hong Huang, Yin-Ju Lai, and Lin I, Chin. J. Phys. **37**, 184 (1999).

[52] A. Melzer, B. Buttenschon, T. Miksch, M. Passvogel, D. Block, O. Arp, and A. Piel, Plasma Phys. Controlled Fusion **52**, 124028 (2010).

[53] A. Melzer, V. A. Schweigert, and A. Piel, Phys. Rev. Lett. **83**, 3194 (1999).

[54] G. A. Hebner, M. E. Riley, and B. M. Marder, Phys. Rev. E **68**, 016403 (2003).

[55] G. A. Hebner and M. E. Riley, Phys. Rev. E **68**, 046401 (2003).

[56] G. A. Hebner and M. E. Riley, Phys. Rev. E **69**, 026405 (2004).

[57] G. A. Hebner, M. E. Riley, and B. M. Marder, IEEE Trans. Plasma Sci. **33**, 396 (2005).

[58] A. A. Samarian and S. V. Vladimirov, Contrib. Plasma Phys. **49**, 260 (2009).

[59] V. V. Yaroshenko, S. V. Vladimirov, and G. E. Morfill, New J. Phys. **8**, 201 (2006).

[60] J. D. E. Stokes, S. V. Vladimirov, and A. A. Samarian, Phys. Lett. A **371**, 145 (2007).

[61] J. D. E. Stokes, A. A. Samarian, and S. V. Vladimirov, Phys. Rev. E **78**, 036402 (2008).

[62] A. K. Mukhopadhyay and J. Goree, Phys. Rev. Lett. **109**, 165003 (2012).

[63] A. K. Mukhopadhyay and J. Goree, Phys. Rev. Lett. **111**, 139902(E) (2013).

[64] M. S. Green, J. Chem. Phys. **25**, 836 (1956).

[65] J. E. Mayer, *Statistical Mechanics*, 2nd ed. (Wiley, New York, 1977), Chap. 9.

[66] D. R. Nicholson, *Introduction to Plasma Theory* (Wiley, New York, 1983), Chap. 4.

[67] B. Liu *et al.*, Phys. Plasmas **16**, 083703 (2009).

[68] W. J. Miloch, J. Trulsen, and H. L. Pécseli, Phys. Rev. E **77**, 056408 (2008).

[69] D. Block, J. Carstensen, P. Ludwig, W. J. Miloch, F. Greiner, A. Piel, M. Bonitz, and A. Melzer, Contrib. Plasma Phys. **52**, 804 (2012).

[70] W. J. Miloch and D. Block, Phys. Plasmas **19**, 123703 (2012).

[71] Y. Feng, J. Goree, and B. Liu, Rev. Sci. Instrum. **78**, 053704 (2007).

[72] Y. Feng, J. Goree, and B. Liu, Rev. Sci. Instrum. **82**, 053707 (2011).

[73] P. Hartmann, Z. Donkó, G. J. Kalman, S. Kyrkos, K. I. Golden, and M. Rosenberg, Phys. Rev. Lett. **103**, 245002 (2009).

[74] Since the fat tail of f_1 is not easily seen when comparing the data points to a Gaussian fit in Figs. 3(c) and 3(d), we fit f_1 to a Tsallis distribution, which would have an exponent $q = 1$ for a Gaussian and $q > 1$ for a fat tail [C. Tsallis, Braz. J. Phys. **29**, 1 (1999); Phys. Rev. E **69**, 038101 (2004)]. For the parallel alignment, the exponent is $q = 1.03$. For perpendicular alignment, we find that $q = 1.05$ for the lower (β) microparticle and $q = 1.10$ for the upper (α).

[75] We calculated the correlation coefficient ρ of $v_x(t)$ and $v_z(t)$ for a given microparticle as their covariance $\langle v_x(t)v_z(t) \rangle$ divided by the product of their standard derivations for $v_x(t)$ and $v_z(t)$. We found that ρ is a very small -0.08 for the upper particle α and only -0.09 for the lower particle β. We also calculated the cross correlation $\langle v_x(t)v_z(t - \tau) \rangle$, which does not reveal any significant relationship of v_x and v_z for a given particle for any lag time τ.